Studying FCC Crystal Properties using the Electron Microscope

Eric Yeung
Department of Physics, University of Toronto, Toronto M5S 1A7, Canada
(Dated: April 5, 2016)

This experiment studied the lattice properties of various specimens using a transmission electron microscope. The lattice structure and lattice parameter of an unknown sample was found by observing the diffraction patterns of elements with the same lattice structure (face-centered cubic– abbreviated FCC); the unknown sample was identified to be copper. The Curie temperature T_c of nickel was found by heating up the nickel sample slowly and observing the temperature at which the domain walls disappeared. The observed T_c was slightly outside the uncertainty for the known value for pure nickel. It was also concluded that the nickel sample displayed paramagnetic behaviour for $T \geq T_c$.

I. INTRODUCTION

A transmission electron microscope (TEM) operates by transmitting an electron beam through a very thin sample. The transmitted electron behaves like a wave with de Broglie wavelength λ and scatters off the atoms in the sample. This scattering produces waves– resulting in constructive and destructive interference. In constructive interference, there is superposition of the waves, resulting in a greater final amplitude. In destructive interference, the waves will cancel out resulting in zero or insignificantly small amplitudes. The result is a diffraction pattern.

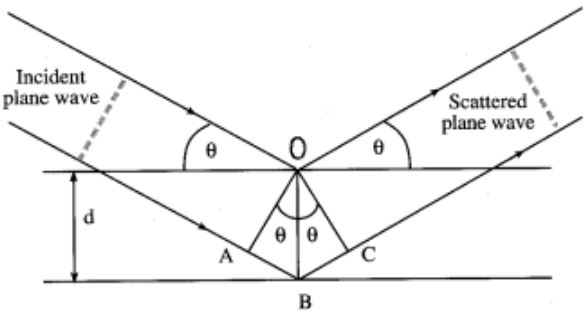

FIG. 1: Bragg diffraction [3].

From [Fig. 1], one can derive Bragg's law. Let θ be the Bragg angle, the angle of the incident electron beam relative to two parallel crystal planes with Miller indices (hkl).

d_{hkl} is the spacing between adjacent lattice planes with Miller indices (hkl), shown by the two horizontal lines in [Fig. 1], such that

$$d_{hkl} = \frac{a}{\sqrt{h^2 + k^2 + l^2}} \tag{1}$$

where a is the lattice parameter, and (hkl) are the Miller indices. The Miller indices represent which planes intersect the axes. For example, the (100) plane intersects only the $\vec{e}_1$ axis while the (011) plane intersects only the $\vec{e}_2$ and $\vec{e}_3$ axes.

From the superposition principle, the constructive interference case results in an electron beam with higher intensity, while the destructive interference case results in a beam with insignificantly small intensity. Following the derivation in [3], constructive interference occurs when ABC is an integer multiple of the wavelength nλ.

$$\begin{aligned} \mathrm{AB} = \mathrm{BC} &= \mathrm{OB}\sin\theta \\ 2\mathrm{OB}\sin\theta &= \mathrm{n}\lambda \end{aligned} \tag{2}$$

and OB is just the interplanar spacing d_{hkl} [3]. Therefore, the condition for constructive interference in the scattering is given by

$$2d_{hkl}\sin\theta = n\lambda \tag{3}$$

This is also known as Bragg's law. When the Bragg condition is satisfied, there will be momentum transfer. The difference in momentum of the incident and diffracted electron beam is a reciprocal lattice vector. The reciprocal lattice is the Fourier transform of the Bravais lattice. The rings visible in this experiment are projections of the Ewald's sphere, the reciprocal lattice of the crystal, onto the plate of the TEM. So the bright areas of the diffraction pattern correspond to constructive interference, while the dark areas correspond to destructive interference.

The relation between the lattice plane spacing and the camera constant K for the diffraction pattern photographs is given by

$$d_{hkl} = n\left(\frac{K}{D}\right) \tag{4}$$

where n is a positive integer, D is the diameter of the ring corresponding to a (hkl) plane, and d_{hkl} is the interplanar spacing [1]. In [Eq. 3] and [Eq. 5], n represents the order of diffraction. However, in electron diffraction, it suffices to consider only the first order of diffraction (i.e. n = 1) because one can deal with higher order diffraction by using multiples of the Miller indices [4]. For example, if one wants to study the second order diffraction from the (111) plane, one just needs to multiply by n = 2. So the first order diffraction from the (222) plane can be studied instead. Therefore, plugging [Eq. 1] into [Eq. 4], the equation for the camera constant becomes

$$K = \frac{a \cdot D}{\sqrt{h^2 + k^2 + l^2}} \tag{5}$$

If the camera constant is known for a certain lattice structure, one can rearrange the equation above to find lattice constants for unknown samples with the same lattice structures.

For ferromagnetic materials, the magnetic moments are aligned and parallel below the Curie temperature T_c. Above

T_c, the material undergoes a phase transition and the magnetic moments become disordered. For paramagnetic materials, the magnetic moments are aligned and parallel above T_c if there is a magnetic field present. Otherwise, the magnetic moments are disordered. These regions of disordered magnetic moments are separated by domain "walls". When the magnetic moments are ordered, the regions disappear because they become homogeneous. The TEM allows observation of the disappearance and appearance of these domain walls, and therefore can be used to find the T_c of a sample.

II. APPARATUS

The TEM used was the Hitachi EM III electron microscope. Unlike a light microscope, the illuminating source is an electron beam, instead of light. Instead of glass lenses, the TEM uses magnets to direct the electron beam. The accelerating voltage used to produce the electron beam was 75 kV. Throughout the experiment, the objective lens current remained constant at 101 mA while the projection lens remained at 71 mA. A firewire camera was used to record the diffraction patterns and domain images displayed on the plates. It was assumed to have an accuracy of 1 pixel. Each pixel represented 1/4.25 millimetres, resulting in an uncertainty of ±0.24mm.

All the samples in this experiment were metals with FCC structure: gold, aluminium, silver, and nickel. This allows us to look at the same set of (hkl) planes, which were (111), (200), (220), and (311) for elements with FCC structure. After putting the respective sample into the TEM, the diffraction patterns were recorded using the camera and labview. Then, the diffraction pattern pictures were read using SciPy's ndimage module [2]. The intensity was then plotted against the x-axis and the peak locations were found. Since the intensity plots are approximately symmetric, the distance between two peaks gives the diameter of a ring. Firstly, the known value of the lattice parameter of gold was used to find the camera constant. Then, [Eq. 5] was used to find the lattice parameters of the other samples.

For observing nickel's domain structure instead of diffraction patterns, the TEM's field of view was changed. The nickel sample was heated slowly from 0.02 mV to 3 mV. The temperature was measured using a type R thermocouple with an uncertainty of ±1.5 °C or ±0.25%. The relative uncertainty was used for the Curie temperature instead of the absolute uncertainty since kelvins were used as the unit.

Using a python program, the thermocouple voltages were converted into temperatures. Equivalently, the sample was heated from 276.89 K to 633.42 K. Pictures were taken around every 30 K. Pictures of the domain structure were also taken when the sample was cooling from 619.56 K to 418.15 K to get a more accurate result of T_c. While the domain walls reappeared as expected, the pictures did not provide any additional insight.

III. RESULTS

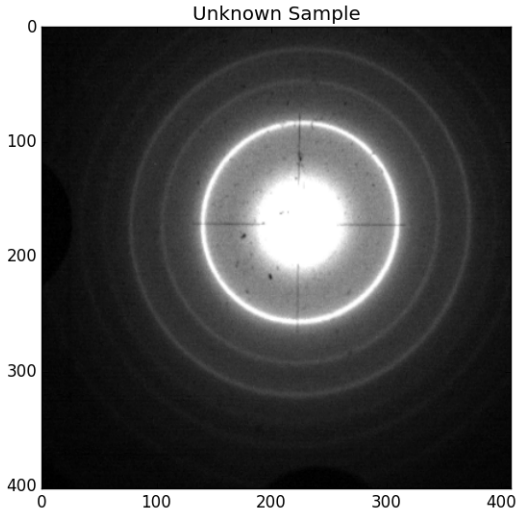

FIG. 2: Diffraction pattern of the unknown sample.

The intensity plots of the diffraction patterns for gold, aluminium, silver, and nickel are omitted. The intensity plot of the diffraction pattern for the unknown sample, [Fig. 2], is shown below in [Fig. 3].

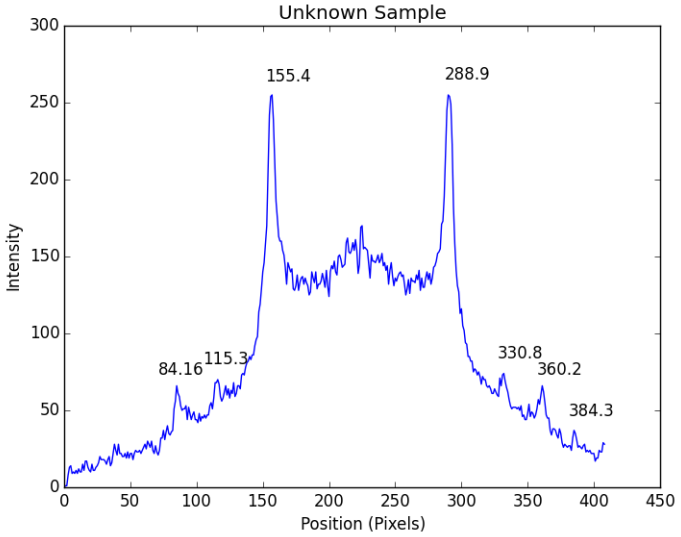

FIG. 3: Location of the intensity peaks in the unknown sample. Note that the peaks for the 4th ring are not well defined. This is because the 4th ring was very dim.

Naturally, in order to see the peaks in the 4th ring better, brighter pictures of the diffraction pattern were taken by increasing the current of the TEM. [Fig. 4] shows the locations of the intensity peaks of the 4th ring.

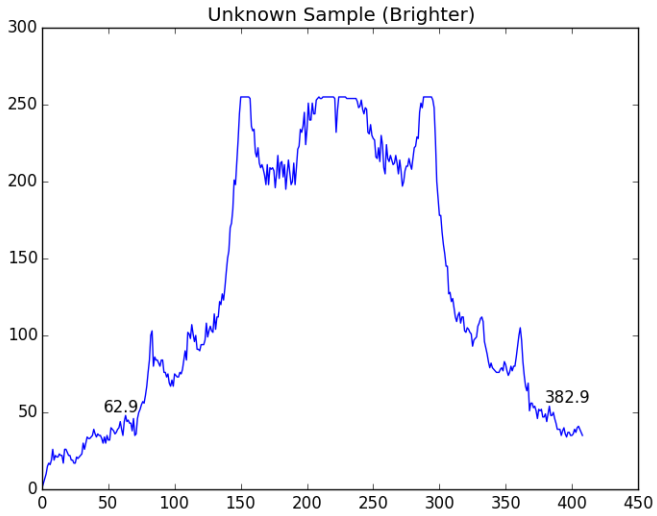

FIG. 4: A brighter diffraction pattern allows the intensity peaks in the 4th ring to appear.

The distance between the peak locations in the intensity plots above give the ring diameters. The diameters of the rings in the diffraction pattern corresponding to the (111), (200), (220), and (311) planes were found.

TABLE I: The diameter of the rings corresponding to the (111) plane.

Element	Diameter (±0.24mm)
Gold	27.47
Aluminum	28.18
Silver	25.55
Unknown	31.41

Using the known lattice parameter of gold a = 0.4079 nm for calibration, and h = k = l = 1, the camera constant was found to be K = (1.617 ± 0.01) nm·mm using [Eq. 5]. The camera constant K was also calculated for the other rings as well but were not used; those results deviated slightly from the one obtained from the ring corresponding to the (111) plane. Therefore, the diameters of the rings corresponding to the other planes are omitted. Since K is a known constant, one can rearrange [Eq. 5] for the lattice parameter a.

The lattice parameter of aluminium was found to be (0.3976 $\pm 3.5 \times 10^{-3}$) nm. The known value for aluminium is 0.4046 nm, which is slightly outside the uncertainty. Silver's lattice parameter was found to be (0.4386 $\pm 3.8 \times 10^{-3}$) nm. The known value for silver is 0.409 nm, which is outside the uncertainty. Since there is very small spread in the uncertainties for aluminium and silver, one can now calculate the lattice parameter of the unknown sample to determine what it is.

The unknown sample's lattice parameter was found to be a = (0.3567 $\pm 3.1 \times 10^{-3}$) nm. Copper has a lattice parameter of 0.3597 nm, so the unknown sample is identified as copper because it's within the uncertainty ($\pm 3.1 \times 10^{-3}$ nm).

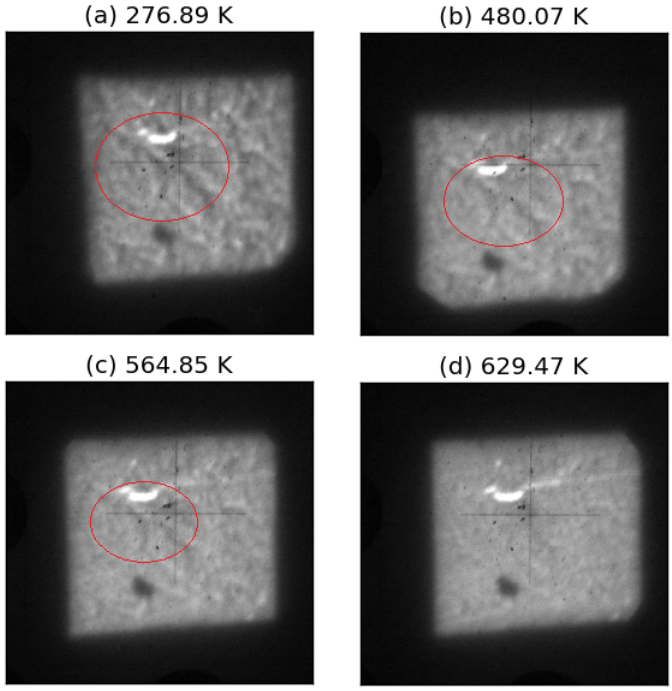

FIG. 5: The magnetic domain structures in nickel. The domain walls are not visible in (d) at the Curie temperature T_c = 629.47 K.

The domain walls that divide different orientations of the magnetic dipoles in nickel can be seen as the "bumps" in [Fig. 5]. The picture, (d) in [Fig. 5], at 629.47 K is "smooth" when the domain walls disappear; all the magnetic dipoles have the same orientation as it increases beyond the Curie temperature, which is found to be T_c = (629.47 ± 1.6) K.

IV. DISCUSSION

In this experiment, the camera constant for any diffraction pattern photograph was calculated using a known value of gold's lattice parameter. Subsequently, this camera constant was used to find the lattice parameter of the unknown sample by rearranging [Eq. 5]. However, it should be noted that one can only use the same set of Miller indices if the unknown sample also had a FCC structure. If the sample was, for example, body-centered cubic (BCC) instead, it would have planes with different Miller indices and one would not be able to use the same camera constant. One would need to recalibrate the camera constant using a known lattice parameter of another element with BCC structure, like chromium.

The Curie point of pure nickel is known to have an empirical value of T_c = 627 K. The value found in this experiment was T_c = (629.47 ± 1.6) K; which is slightly outside the uncertainty. Since Nickel is paramagnetic when $T \geq T_c$, the magnetic moments are ordered in the presence of an applied magnetic field produced by the TEM. This is consistent with what is seen in [Fig. 5]. The main sources of error in this part of the experiment were the infrequent pictures. The pictures were taken every 30 K; a third of this would be significantly better in determining T_c as the domain walls seemed to disappear before 629.47 K.

V. CONCLUSION

Using the transmission electron microscope to find the lattice parameter of the unknown sample a = $(0.3567 \pm 3.1\times10^{-3})$ nm, the unknown metal was identified to be copper which has lattice parameter a = 0.3597 nm.

After studying the domain structure of nickel, its Curie temperature was found to be $T_c = (629.47 \pm 1.6)$ K, which deviates slightly from the known Curie temperature of pure nickel $T_c = 627$ K. The domain walls in the nickel sample were also absent for $T \geq T_c$, which implies paramagnetic behaviour.

[1] B. W. Statt, "Electron Microscope Lab Manual" (2015), 2-13

[2] Jones E, Oliphant E, Peterson P, et al. SciPy: Open Source Scientific Tools for Python, 2001-, http://www.scipy.org/[Online; accessed 2016-03-18].

[3] "Introduction to TEM", UC Riverside. http://cfamm.ucr.edu/documents/tem-intro.pdf

[4] P.J. Goodhew and J. Humphreys, "Electron Microscopy and Analysis", 3rd Ed. (CRC Press, Boca Raton, FL, 2000), pp. 42-43.